9C.6 Asymmetries of Tropical Cyclone Convection in Different Intensity Change Stages as Derived from Satellite 85 and 37 GHz observations

Yongxian Pei* and Haiyan Jiang
Department of Earth and Environment, Florida International University, Miami, Florida

1. Introduction

The physical processes associated with tropical cyclones (TCs)' rapid intensification (RI), which is usually defined as 24-h intensity increase ≥ 30 kt (Kaplan and DeMaria 2003), remain unsolved. Predicting these events is one of the most challenging aspects for TC forecasters. It is well agreed that a favorable pre-existing environmental condition is necessary for RI (Hendrickset al. 2010). However, it is not well understood about the roles of inner core precipitating systems and intense convective events and their interaction with the vortex. Observational and modeling studies (Kelley et al. 2004; Montgomery et al. 2006; Rogers 2010; Jiang 2012) have linked asymmetric deep convection such as hot towers and convective bursts in the inner core with TC intensification in general and RI in particular. However, many theoretical studies have shown that a TC intensifies through an axisymmetric mechanism (Ooyama 1969; Shapiro and Willoughby 1982), and the azimuthally averaged latent heating release is deemed much more important for the vortex intensification than asymmetric heating (Nolan et al. 2007). Recently, Kieper and Jiang (2012) documented a distinctive ring pattern around the TC center in the 37 GHz composite passive microwave images to be an indicator of subsequent RI. The ring pattern appears as a bright cyan color ring (pink color may be part of the ring) around the storm center on the 37 GHz color composite product developed by the Naval Research Laboratory (NRL, Lee et al. 2002). The product is generated using 37 GHz Polarization Corrected brightness Temperatures (PCTs, Spencer et al. 1989, Cecil et al. 2002) and 37 GHz horizontally polarized (37H) and vertically polarized (37V) brightness temperatures. A comparison with simultaneous radar observations shows that the cyan color region mainly contains shallow convective rain without ice while the pink color region mainly contains stratiform or convective rain with ice. Kieper and Jiang (2012)'s results suggest that the degree of rainfall and convective asymmetry is related to TC intensity change, especially RI. However, in Kieper and Jiang (2012), the ring was defined subjectively. To further link the degree of asymmetry of precipitation and convection with TC intensity change, it is necessary to quantify the asymmetry. This research will quantitatively examine the climatology of precipitation and convection asymmetries in TCs and their relationship to TC intensity changes using a 14-year satellite database to finally examine whether the degree of symmetry of precipitation and convection is a good indicator of TC intensification.

2. Data and Method

The main tool that will be used is the Tropical Rainfall Measuring Mission (TRMM) Tropical Cyclone Precipitation Feature (TCPF) database (Jiang et al. 2011), which contains 14 full years (1998-2011) of TRMM observations (23,102 individual TRMM overpasses of 1146 TCs). The TCPF database was developed by the PI in collaboration with Zipser's group at the University of Utah. This research will mainly use level-1 TCPF data, which are orbital data containing collocated pixel-by-pixel observations and retrievals from TRMM Microwave Imager (TMI), Precipitation Radar (PR), Visible and Infrared Scanner (VIRS), and Lightning Imaging System (LIS).

For each TRMM TC overpass, storm parameters are added in based on a linear interpolation from the "best track" database, which is an archived 6-h post analysis product from the National Hurricane Center (NHC) for TCs in the North Atlantic and Eastern North Pacific basins and Joint Typhoon Warning Center (JTWC) for TCs in other basins. TCs in six different TC-prone basins are separated: north Atlantic (ATL), East

**Corresponding author address:* Yongxian Pei, Dept. of Earth and Environment, Florida International University, Miami, FL 33199. Email: ypei002@fiu.edu

Central Pacific (EPA), Northwest Pacific (NWP), North Indian Ocean (NIO), South Indian Ocean (SIO), and South Pacific (SPA). A series of storm parameters are calculated from the best track information, which include: storm center location, land/ocean flags of the current, future 6, 12, 18, and 24-h TC center, current TC maximum wind speed, storm motion direction and translation speed, and future 24-h wind speed, etc. In order to determine environmental conditions, the ECMWF Interim reanalysis data have been interpolated into each TRMM TC overpass.

The TRMM satellite was launched in November of 1997 (Simpson et al. 1988) and remains operational at the time of this writing. During August 2001 its altitude was boosted from 350 km to 402 km to reduce drag and therefore increase its lifetime in orbit. The TMI has a 760 km swath width before the TRMM boost and 878 km swath width after boost. In this research, the 2124 overpasses in the northern hemisphere with the storm's core region (200km radius from the storm center) well-observed by the TRMM Microwave Imager (TMI) sensor are manually selected as shown in Table 1. All of these selected overpasses are rotated relative to the direction of environmental vertical wind shear.

The environmental criteria are added into the TRMM database from two other datasets. The SST data is derived from the 0.25 degree Reynolds daily SST grid point nearest to the TC center (Reynolds et al. 2007). The total precipitable water (TPW) data and vertical wind shear data are derived from the ECMWF interim reanalysis dataset (Simmons et al. 2006). The TPW data was averaged in the inner 250km around the TC center. To calculate the vertical wind shear, the 200-hPa and 850-hPa wind vectors between 500 and 750 km from the storm center are averaged.

All of the selected overpasses are divided into four intensity change categories. They are separately: rapidly intensifying (RI), slowly intensifying (SI), neutral (N), weakening (W), which are from the four basins in northern hemisphere. And the initial maximum intensity at the time of each overpass is between 33 and 95 knots. A tropical depression (intensity lower than 33 knots) represents only a small portion of RI storms (Kaplan et al. 2010). Category 3-5 hurricanes generally intensify and weaken through eyewall replacement cycles (Willoughby et al. 1982), which are not included in this study. To rule out the overpasses with unfavorable conditions, we use the following environmental condition criteria to refine the 2124 overpasses: SST > 26 °C , mean inner-250 km TPW > 50 mm, vertical wind shear < 13 m s^{-1}, and storm motion <10 m s^{-1}.

Similar to Lonfat et al. (2004), 10-km-wide (20-km-wide) annuli around the TC center are used to compute the spatial asymmetry of 85 GHz PCT (37 GHz PCT, 37H, and 37V). In each annulus, the Fourier coefficients are computed using the following equation (Stull 1987):

$$a_n = \frac{1}{N}\sum_{k=0}^{N-1} R(k)\cos(2\pi nk / N)\text{, and } b_n = -\frac{1}{N}\sum_{k=0}^{N-1} R(k)\sin(2\pi nk / N),$$

where *R(k)* is each individual rain or brightness temperature, n is the wavenumber, N is total number of points being analyzed in each annuli, and k is index of each point. According to Zhu (et al. 2013), the total perturbation energy and the fraction of it contributed by each wavenumber in each annulus around the storm center can be computed from above Fourier coefficients. Table 2 shows the percentage contribution of each wavenumber to the total perturbation energy for 85 PCT and 37 PCT derived from all 2124 well-observed TMI overpasses. Note that contribution from wavenumber >5 are accumulated. From Table 2, we can see that over 60-70% of total energy is from wavenumber 1 and 2. Therefore, in this proposed research, we plan to analyze the dominant asymmetries (*M*), which is the sum of the wavenumber 1 and 2 amplitude divided by the mean rain rate or brightness temperature calculated over the entire annulus.

3. Results

The composite images in Figure 1 show the 85 PCT asymmetries in different TC intensity change categories inside the innermost 200 km region around the TC center. The images are composited by rotating shear directions of all the cases pointing upward. The black solid line marked by 0.0 in each panel represents the zero value of asymmetry. These shear relative images are generated by the quadrant approach (Chen et al. 2006). Each quadrant: upper-left, upper-right, lower-left, and lower-right quadrants are defined as downshear-left, downshear-right, upshear-left, and upshear-right.

Figure 1 shows the composite asymmetries of 85GHz PCT . For the parameter of 85 GHz PCT and 37 GHz PCT, the negative asymmetries region is where contributes to lowering down the brightness temperature. In the figure, the warm color shows where should be concerned and those are negative values. The lower the 85 GHz PCT or 37 GHz PCT is, the more ice scattering there will be. The asymmetry defined as wave-number 1 plus 2 together divided by azimuthal mean shows similar distribution in all categories, basically concentrates downshear-left as Chen et al. 2006. But for the RI composite image, it shows differences from other categories. First, the inner 50 km area shows the asymmetries whose absolute values are near to zero, which means the RI cases have more symmetric 85 GHz PCT distribution in the inner 50 km. Second, the minimum amplitude of asymmetries in the RI composite is smaller than those in the other categories. And the area of smaller (negative) amplitude in RI composite is much smaller than other categories. The areas of low amplitude region (redder color) in the composites of different categories rank as RI<SI<N<W. For the 37 GHz composite asymmetries, it shows similar features as 85 GHz PCT's (not shown). That means the RI cases are less asymmetric not only in the inner core regions but also in the inner rain band and outer rain band regions.

The composite asymmetries of 37V are shown in the Figure 2. For the parameter of 37V and 37H, the positive asymmetries region contributes to enhancing the brightness temperature. And the higher the 37V and 37H, the more light or moderate precipitation there will be. Similarly, the warm color region that shows positive asymmetries are where need to be concerned. The asymmetries concentrate mostly in the region of downshear-left. The inner 100 km for RI cases composite image has more blue color, which also means that the distributions of 37V brightness temperature for RI cases are more symmetric. That also means for the RI cases, the moderate rain distributes symmetrically inside the innermost 100 km region. The maximum asymmetry value is smaller than those in the other categories. The 37H composite figures show similar features (not shown).

In the Figure 3, it shows the radial distribution of azimuthal mean for different parameters. For the 85 GHz and 37 GHz PCT, the azimuthal mean radially smaller than those in the other categories. This means the RI cases averagely have more convection than the other categories. For 37H and 37V, the azimuthal mean values of RI cases are radially greater than other categories, which means the RI cases have more moderate precipitation.

In the Figure 4, the radial maximum or minimum asymmetries are shown. RI cases radially have bigger minimum asymmetries for The 85 GHz and 37 GHz PCT, which means the dominant wave-numbers contribution to lowering down the PCTs is small in RI cases indicating RI cases have more symmetric convection distribution. Also RI cases radially have smaller maximum asymmetries for 37H and 37V, which means that the dominant wave-numbers contribution to increasing the brightness temperature is small in RI cases. The RI cases have more symmetric precipitation distributions.

4. Conclusion

The results consistently show that RI storms have stronger convective intensity and rainfall intensity on average, especially in the inner core region. Asymmetries concentrate in the downshear-left for all tropical cyclones. Both convection and precipitation are more symmetric for RI cases and have lower maximum amplitude than all other intensity change categories.

Reference

Cecil, D. J., E. J. Zipser, and S. W. Nesbitt, 2002: Reflectivity, ice scattering, and lightning characteristics of hurricane eyewalls and rainbands. Part I: Quantitative description. *Mon. Wea. Rev.*, **130**, 769-784.

Chen, S. S., J. A. Knaff, F. D. Marks, 2006: Effects of Vertical Wind Shear and Storm Motion on Tropical Cyclone Rainfall Asymmetries Deduced from TRMM. *Mon. Wea. Rev.*, **134**, 3190–3208.

Hendricks, E. A., M. S. Peng, B. Fu, and T. Li, 2010: Quantifying environmental control on tropical cyclone intensity change. *Mon. Wea. Rev.*, **138**, 3243-3271.

Jiang, H., C. Liu, and E. J. Zipser, 2011: A TRMM-based tropical cyclone cloud and precipitation feature database. *J. Appl. Meteor. Climatol.* **50**,1255-1274.

Jiang, H., 2012: The relationship between tropical cyclone intensity change and the strength of inner core convection. *Mon. Wea. Rev*., **140**, 1164-1176.

Kaplan, J., and M. DeMaria, 2003: Large-scale characteristics of rapidly intensifying tropical cyclones in the north Atlantic basin. *Wea. Forecasting*, **18**, 1093–1108.

Kelley, O. A., J. Stout, and J. B. Halverson, 2004: Tall precipitation cells in tropical cyclones eyewalls are associated with tropical cyclone intensification. *Geophys. Res. Lett*., **31**, L24112, doi: 10.1029/2004GL021616.

Kieper, M., and H. Jiang, 2012: Predicting tropical cyclone rapid intensification using the 37 GHz ring pattern identified from passive microwave measurements. *Geophys. Res. Lett.*, **39,** L13804, doi:10.1029/2012GL052115.

Kummerow, C., W. S. Olson, and L. Giglio, 1996: A simplified scheme for obtaining precipitation and vertical hydrometeor profiles from passive microwave sensors. *IEEE Transactions on Geosci. and Remote Sensing.* **34**, 1213-32.

Lee, T. F., F. J. Turk, J. Hawkins, and K. Richardson, 2002: Interpretation of TRMM TMI images of tropical cyclones. *Earth Interactions*, **6**, 1-17.

Lonfat, M., F. D. Marks, and S. S. Chen, 2004: Precipitation distribution in tropical cyclones using the tropical rainfall measuring mission (TRMM) microwave imager: A global perspective. *Mon. Wea. Rev.*, **132**, 1645-1660.

Montgomery, M. T., M. E. Nicholls, T. A. Cram, and A. B. Saunders, 2006: A vortical hot tower route to tropical cyclogenesis. *J. Atmos. Sci.*, **63**, 355–386.

Nolan, D. S., Y. Moon, and D. P. Stern, 2007: Tropical cyclone intensification from asymmetric convection: energetics and efficiency. *J. Atmos. Sci*., **64**, 3377–3405.

Ooyama, K., 1969: Numerical simulation of the life cycle of tropical cyclones. *J. Atmos. Sci.*, **26**, 3–40.

Rogers, R. 2010: Convective-scale structure and evolution during a high-resolution simulation of tropical cyclone rapid intensification. *J. Atmos. Sci.*, **67**, 44–70.

Shapiro, L. J., and H. E. Willoughby, 1982: The response of balanced hurricanes to local sources of heat and momentum. *J. Atmos. Sci.*, **39**, 378-394.

Simpson, J., R. F. Adler, and G. R. North, 1988: A proposed Tropical Rainfall Measuring Mission (TRMM) satellite. *Bull. Amer. Meteor. Soc*, **69**, 278–295.

Spencer, R. W., H. M. Goodman, and R. E. Hood, 1989: Precipitation retrieval over land and ocean with the SSM/I: Identification and characteristics of the scattering signal. *J. Atmos. Oceanic Technol*, **6**, 254–273.

Table 1. The number of TMI well-observed TC overpasses each basin and each intensity change category.

	ATL	EPA	NWP	NIO	TOTAL
RI	33	27	85	5	150
SI	155	93	239	19	506
N	332	167	290	34	823
W	166	181	279	19	645
TOTAL	686	468	893	77	2124

Table 2. The normalized power spectra for 85GHz PCT and 37GHz PCT from wavenumber 1 to 5 and more than 5 in percentage

$E(n)$ (%)	$n=1$	$n=2$	$n=3$	$n=4$	$n=5$	$n>5$
PCT85	36.7	16.0	8.3	6.5	4.4	28.1
PCT37	34.5	15.2	8.5	6.8	4.8	30.2

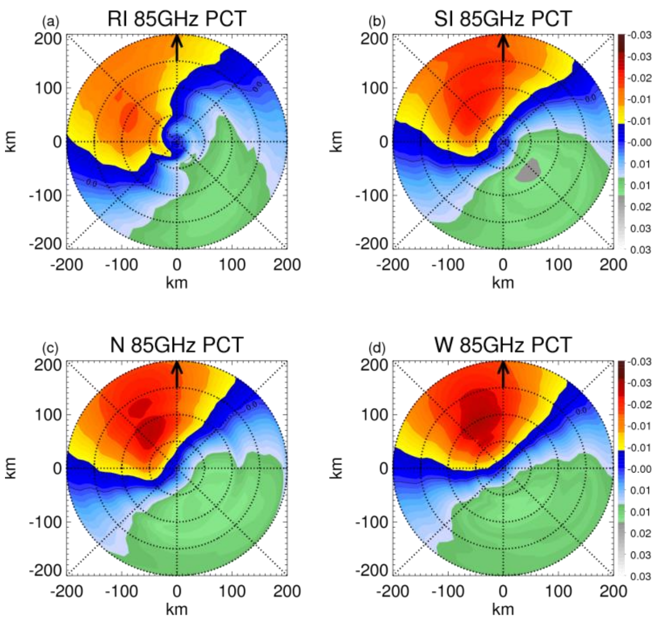

Figure 1. The dominant wavenumber 1+2 85 GHz PCT asymmetry relative to the 200-850-hPa environmental vertical wind shear in different intensity change categories. The analysis is done in a cylindrical coordinate. The shear vector is pointed to the top in all panels. The color scale represents the fraction of dominant wavenumber (1+2) asymmetry normalized by the azimuthal mean value.

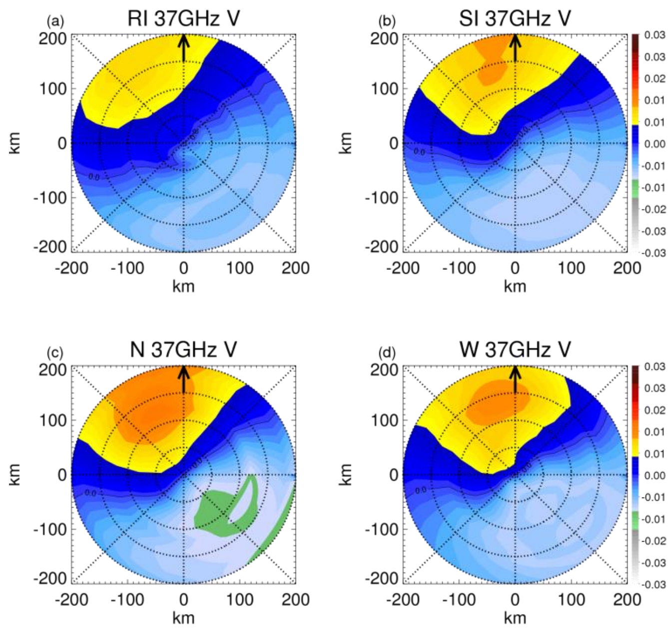

Figure 2. Same as Figure 1 but for 37V asymmetry.

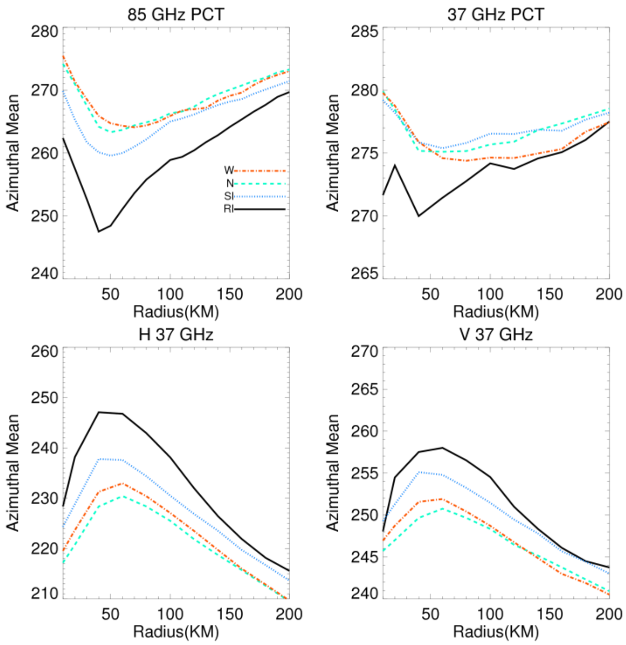

Figure 3. Radial distribution of azimuthal mean value of a) 85 GHz PCT, b) 37 GHz PCT, c) 37 H and d) 37 V.

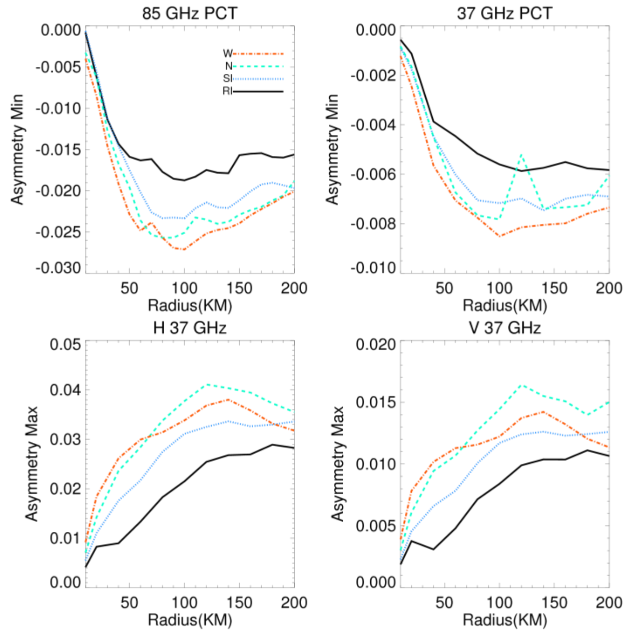

Figure 4. Radial distribution of azimuthal maximum or minimum value of a) 85 GHz PCT, b) 37 GHz PCT, c) 37 H and d) 37 V.